

Protective and therapeutic effects of *Pilose antler* against kidney deficiency-induced osteoporosis

Cong Ren¹, Wei Gong², Feng Li^{1*}, Ming Xie^{1*}¹ Department of Pharmacy, Liaoning University of Traditional Chinese Medicine, Dalian, Liaoning, China² Affiliated Hospital of Liaoning University of Traditional Chinese Medicine, Shenyang, Liaoning, China

*Correspondence to: zhanglijiyi@163.com, x6m6@163.com

Received April 1, 2019; Accepted June 4, 2019; Published June 30, 2019

Doi: <http://dx.doi.org/10.14715/cmb/2019.65.5.4>

Copyright: © 2019 by the C.M.B. Association. All rights reserved.

Abstract: This study was carried out to evaluate the preventive and curative effects of *Pilose antler* against osteoporosis due to *kidney deficiency*, and investigate its potential mechanism of action. A model of osteoporosis due to *kidney deficiency* was established in rats using bilateral ovariectomy. *Pilose antler* polypeptide (PAP), *Pilose antler* polysaccharide (PAP'), and their mixture (PAP+PAP') were separately administered to the rats for 12 weeks, with *progynova* and *xianlingubao* tablets (XLGB) as the positive control groups. We determined the bone mineral density (BMD) and uterus Index of the rats. Osteoblastic bone metabolism-related indices in serum and bone tissue were measured with ELISA. Western blotting and RT-PCR were used to investigate the protein and mRNA expressions of Bmp-2, Smad1, Smad5, Runx2 in bone tissue. The morphology of bone tissue was determined using immunohistochemical methods. Compared with control group, PAP, PAP', PAP+PAP' increased BMD and regulated bone metabolism indices in serum and bone tissue. Treatment with *Pilose antler* up-regulated the mRNA and protein expressions of Bmp-2, Smad1, Smad5 and Runx2. Immunohistochemical staining showed that Bmp-2, Smad1, Smad5 and Runx2 were stained brown, indicating that all of them were positive. There were abnormal changes in the protein expressions of Bmp-2, Smad1, Smad5 and Runx2 in bone tissue, which may be an important mechanism underlying the development of *kidney deficiency* osteoporosis. Moreover, PAP, PAP' and PAP+PAP' had some preventive effects on osteoporosis, probably via the activation of the Bmp-2/Smad1 and Smad5/Runx2 signaling pathways through induction of high expressions of their mRNAs and proteins.

Key words: *Pilose antler* polypeptide; *Pilose antler* polysaccharide; Osteoporosis; Kidney deficiency; Traditional Chinese Medicine (TCM).

Introduction

Western medicine defines osteoporosis as a disease characterized by a decrease in bone mass and deterioration of the bone microstructure (1), resulting in increased brittleness of bone and a systemic skeletal disorder that is prone to bone fractures (2). Although there is no osteoporosis in TCM, the clinical manifestations and pathogenesis of osteoporosis in the TCM are attributed to the "bone sputum" category of TCM (2,3). According to TCM theory, kidney deficiency is the key to the pathogenesis of osteoporosis (4). The main bone marrow for congenital kidney deficiency is the lack of kidney essence. In bone marrow dystrophy, there may be low back pain, knee osteoporosis and other osteoporosis symptoms. In TCM, the kidneys are involved in various functions such as endocrine, neural, immune, and metabolic, and they play various roles in regulating the physiological functions of the body. Studies (5) have shown that the hypothalamic-pituitary-thyroid hypofunctions of the three target glands (thyroid gland, adrenal gland, and gonadal gland) in patients with kidney deficiency are dysfunctional, with reduced hormonal levels and decreased osteogenic function, resulting in a decrease in bone tissue content per unit volume (5). Kidney-invigorating herbs inhibit or correct dysfunctions in the hypothalamic-pituitary-gonadal axis and increase the activity and quantity of osteoblasts.

It has now been established that when ovarian function is low, the ability to synthesize and secrete estrogen is significantly reduced, resulting in insufficient estrogen, which leads to enhanced bone remodeling and enhanced bone resorption. Bone destruction is far greater than bone formation, resulting in osteoporosis. This theory has important guiding significance in experimental research and clinical treatment of osteoporosis. The most classic animal model (6) for osteoporosis research can be successfully established using the method of ovariectomy (7). Hormonal prevention of postmenopausal osteoporosis, and treatment constitute the most recognized strategies for managing osteoporosis (8).

However, the American Disease Prevention Task Force recommends that estrogen be used for the prevention of osteoporosis, preferably for less than 3 years. The Menopause Group of the Obstetrics and Gynecology Branch of the Chinese Medical Association has recommended that the use of estrogen should not exceed 2 years. The adverse effects of estrogens are mainly postmenopausal vaginal bleeding, increased incidence of breast cancer, endometrial cancer, and increased incidence of deep vein thrombosis and pulmonary embolism. Therefore, TCM is safer and better alternative for the prevention and treatment of postmenopausal osteoporosis (9).

Pilose antler, one of the most prized traditional Chinese herbal medicines (Latin name: *Cornu Cervi*

Pantotrichum), has been used in traditional oriental medicine for over 2,000 years. It is used for invigorating the kidney yang, tonifying the essence and blood, and for strengthening muscles and bones (10). Preliminary studies have shown that *Pilose antler* prevents and cures osteoporosis due to kidney deficiency in the rat (11). In this study, the therapeutic effect of *Pilose antler* on osteoporosis due to kidney deficiency was investigated. Modern molecular biology techniques were used to determine the regulatory roles of related proteins in the Bmp-2/ Smad1 and Smad5/Runx2 signaling pathways in osteoporosis therapy so as to unravel the possible mechanism of action involved.

Materials and Methods

Materials

Pilose antler polypeptide (PAP) was extracted using enzymatic hydrolysis method, and the extract was purified with membrane separation technology. The molecular weight was less than 3KD, and the content of PAP was about 17.5%. Crude *Pilose antler* polysaccharide (PAP') was extracted with water and alcohol precipitation, and was de-proteinated. Then, it was decolorized using hydrogen peroxide (H₂O₂), and the refined polysaccharide was washed with anhydrous ethanol, petroleum ether and acetone.

Reagents and equipment

The drugs/reagents used, and their manufacturers and models (in brackets) were: *Progynova* (Bayer Pharmacy, Germany, batch No. 287A); *XianLingGuBao* tablet (XLGB, Guizhou Tongjitang Pharmaceutical Co Ltd, No. 160709); PrimeScript® RT reagent Kit with gDNA Eraser (Takara, DRR047A), and SYBR® Premix Ex Taq™II (Tli RNaseH Plus, Takara, RR820A). Smad 1 ELISA kit (AE91647Ra 2017.06); Smad 5 ELISA kit (AE91655Ra 2017.06); Runx 2 ELISA kit (AE90170Ra 2017.06); Bmp-2 ELISA kit (AE90181Ra 2017.06); BGP ELISA kit (AE909370Ra 2017.06), and ALP ELISA kit (AE91640Ra 2017.06), purchased from AMEKO. The equipment used were Multifunctional Microplate Reader (Infinite M2000, TECAN, Austria), Low Temperature High Speed Centrifuge (MR1822, France Jouan SA), Fluorescent quantitative PCR instrument (Stratagene Mx3000P, Agilent Germany), Protein nucleic acid analyzer (DU640, Backman, USA), and XR-36 dual energy X-ray bone density instrument (NORTHLAND, USA).

Animals and animal grouping

Female SD rats (12 weeks of age, weighing 230-270g) were purchased from Liaoning Changsheng Biotechnology Co., Ltd (laboratory animal licence number was C-LN2017040722). The experiment was conducted according to the Guide for Care of Laboratory Animals. Except for the normal control group, after 7-day modeling, survived ovariectomized rats were randomly divided into 8 groups according to their body weight: model control group, western medicine positive control group given *progynova* suspension containing estradiol valerate at a dose of 0.025 mg·mL⁻¹; Traditional Chinese Medicine (TCM) positive control group given XLGB (0.045g·mL⁻¹); PAP + PAP' group given 0.0175 g·mL⁻¹

+ 0.005 g·mL⁻¹ PAP'; low-dose PAP GROUP (0.0175 g·mL⁻¹); high-dose PAP group (0.1575 g·mL⁻¹); low-dose PAP' group (0.005 g·mL⁻¹); and high-dose PAP' group (0.045 g·mL⁻¹). Each group had 10 rats. The drugs were intraperitoneally injected into each rat right after the operation, except for the normal control and model control groups.

Establishment of a model of osteoporosis due to kidney deficiency

The rats were anaesthetized with 10 % chloral hydrate (3.5mL/kg) and bilateral ovaries were removed. There was no operation in the normal control group. After the operation, the rats were subjected to intramuscular injection of penicillin at a dose of 1.6 mL/kg (800,000U/4 mL saline) for 3 days.

Specimen collection and preservation

Before blood collection, the rats were fasted for 24 h and were anaesthetized with intraperitoneal injection of 10 % chloral hydrate (300 mg/kg). Blood was obtained from the abdominal aorta 2 h after the last administration of the drug. The serum obtained after centrifugation of the blood for 30 min at 3000 rpm was preserved at -70 °C prior to use.

The femura (with caput femoris) were removed and washed with 0.9 % NaCl, wrapped with wet gauze, and then with aluminum foil, and kept frozen at -70°C prior to use.

Determination of bone mineral density

Bone mineral density (BMD) of the isolated rat femura was measured using XR-36 dual energy densitometer and "The Small Subject Scout Scan" software at a scanning width of 15 cm (the length could be adjusted arbitrarily), scanning speed of 40 mm·sec⁻¹, and resolution of 1.0 x 1.0 mm. The BMD was automatically calculated and expressed as bone mineral content per unit area (g·cm⁻²).

Determination of uterus index

The wet weight of the uterus was obtained using an electronic balance, and uterus index was calculated by dividing the wet weight of the uterus with the body weight of the rat.

Determination of bone metabolism-related indices in serum

Estradiol (E2), ALP, BGP, BMP-2, tartrate-resistant acid phosphatase (TRAP) and peroxisome proliferator activated receptor γ -2 (PPAR γ -2) were assayed in the rat serum using ELISA kits in line with the manufacturer's instructions.

Determination of bone metabolism-related proteins in bone tissue

The femura were weighed and ground with normal saline in ice-cold water bath to form 10 % bone tissue homogenate. After centrifugation, the supernatant was kept at -70 °C prior to use for the assay of bone alkaline phosphatase (BALP), BGP, BMP-2, Smad1, Smad5, Runx2 and transforming growth factor- β 1 (TGF- β 1) with ELISA.

Table 1. Sequences of the primers used for qRT-PCR.

Gene	GeneBank Number		Primer sequence (5'-3')	Gene fragment
Bmp-2	NM_017178	F	5'-CTGCGGTCTCCTAAAGGTCG-3'	180bp
		R	5'-ACTCAAACCTCGCTGAGGACG-3'	
Smad1	NM_013130	F	5'-GCAGTTGCTTACGAGGAACC-3'	223bp
		R	5'-GGTGGACTCCTTTCCCGATG-3'	
Smad5	NM_021692	F	5'-AGCAGAGATGTTTCAGCCTGT-3'	213bp
		R	5'-GCCTGGTGTTCCTCGATGGTT-3'	
Runx2	NM_001278483	F	5'-GCCTTCAAGGTTGTAGCCCT-3'	178bp
		R	5'-TGAAACTCTTGCCTCGTCCG-3'	
β-actin	NM_031144	F	5'-CGCGAGTACAACCTTCTTGC-3'	70bp
		R	5'-CGTCATCCATGGCGAACTGG-3'	

Determination of bone metabolism-related genes in bone tissue using RT-PCR

The femura were ground, and the total RNA was extracted according to the manufacturer’s instructions of the Prime Script RT reagent Kit. The total DNA was reverse transcribed to cDNA with gDNA Eraser Kit, and subjected to qRT-PCR. The primers were designed using Primer-BLAST (12). The primer sequences are shown in Table 1. β-Actin was used as a reference. The relative expression of mRNA in each sample was calculated using the formula below (13):

$$\text{ratio} = \frac{(1 + E_{\text{target}})^{\Delta Ct_{\text{target}}(\text{control-sample})}}{(1 + E_{\text{ref}})^{\Delta Ct_{\text{ref}}(\text{control-sample})}}$$

where E_{target} is the amplification efficiency of target gene, E_{ref} is amplification efficiency of reference genes, ΔCt is the difference between the control and sample groups.

Determination of bone metabolism-related proteins in bone tissue using western blotting

A 10 % bone tissue homogenate was prepared by grinding the femora in normal saline. In line with the specification of BCA-200 protein quantitative kit, the total protein was extracted and subjected to SDS-PAGE electrophoresis, followed by transfer of the separated proteins to polyvinylidene membrane, blocking, and incubation with conjugated secondary antibody. Gel imaging system analysis software was used to determine the gray value of the protein. The levels of the expression of the proteins were expressed as the ratios of the specific protein gray values to that of β-actin, using densitometric scanning analysis.

Immunohistochemistry

In this assay, the tissues were fixed in 4 % paraformaldehyde /0.1 MPBS (pH 7.0 - 7.6) for 30 to 60 min, and then embedded in paraffin. The tissues were sliced, dewaxed and hydrated, followed by inactivation of endogenous peroxidase with freshly-prepared 3 % H₂O₂ in distilled water (1:10). The antigens were repaired by heating, and were washed 2-3 times with PBS, followed by blocking with 5 % BSA solution for 20 min at room temperature. They were then incubated with appropriately diluted antibody (mouse or rabbit IgG) at 37 °C for 1 h or at 4°C overnight, followed by washing 2 – 3 times with PBS (pH 7.2-7.6). Biotinylated goat anti-mouse IgG was added and incubated at 20 -37 °C for 20 min, followed by washing 4 times with PBS (pH 7.2-7.6),

each for 5 min. Then, color development was effected with DAB reagents in line with the procedures outlined in the DAB kit.

Statistical analysis

All data are expressed as mean ± standard deviation. Statistical analysis was performed with one-way analysis of variance (ANOVA) using SPSS 16.0 software. Arithmetic means, standard deviation (SD) and 95% confidence intervals were calculated for each experimental group.

Results

Results of BMD in rats in vitro

Compared with normal group, BMD in the model group was decreased significantly, indicating that ovariectomy rat model of osteoporosis due to *kidney-deficiency* was successfully established. After 12 weeks of continuous administration of PAP, PAP', PAP+PAP', the BMD of the rats were significantly increased. Moreover, PAP, PAP', PAP+PAP' increased BMD, but the effect of PAP+PAP' was significantly higher than that of any other group. Thus, PAP strengthened the bone and so has potential for use in the treatment of osteoporosis. These results are shown in Table 2.

Results of Uterus Index

The uterus of rats in normal group was healthy. After the operation, the uteri of rats in model group were significantly atrophied. As shown in Table 2, the uterus index values of the other groups were significantly

Table 2. BMD and uterus index of rats ($\bar{x} \pm s$, n = 10).

Group	BMD (g·cm ²)	Uterine Index (%)
Normal	0.1955±0.02325	2.2558±0.2132
Model	0.1363±0.0233 ^Δ	0.2017±0.0203 ^Δ
Progynova	0.2679±0.0873 [#]	0.2679±0.0873
XLGB	0.3394±0.1555 [#]	0.2355±0.0298
PAP+PAP'	0.3745±0.0197 ^{*#}	0.3514±0.0129
Low dose PAP	0.2874±0.0774 ^{*#}	0.1839±0.0239
High dose PAP	0.3359±0.1351 ^{*#}	0.2045±0.0337
Low dose PAP'	0.343±0.1525 ^{*#}	0.2007±0.0452
High dose PAP'	0.416±0.149 ^{*#}	0.2552±0.0358

* $p < 0.05$, compared with the positive group, # $p < 0.05$, compared with the model group; ^Δ $p < 0.05$, compared with the normal control group.

smaller than that of the normal group. Compared with model group, there was no significant difference in uterine index between the positive medicine group, PAP group, PAP' group, PAP+PAP' group ($p > 0.05$).

Effect of treatments on serum markers of bone metabolism in rats

Table 3 shows that PAP enhanced the levels of ALP, BGP, BMP-2 and E2, and lowered the levels of TRAP and PPAR γ -2, indicating that *Pilose antler* suppressed osteoporosis in a two-way process involving promotion of bone reconstruction and inhibition of bone resorption.

Effect of treatments on bone metabolism-related proteins in bone tissue

The levels of BALP, BMP-2, Smad 1, Smad 5, Runx 2, TGF- β 1 in the model group were significantly decreased compared with the normal group ($p < 0.05$).

However, following treatment with PAP, activity of BALP and levels of BMP-2, Smad 1, Smad 5, Runx 2, TGF- β 1 were significantly enhanced (Table 4).

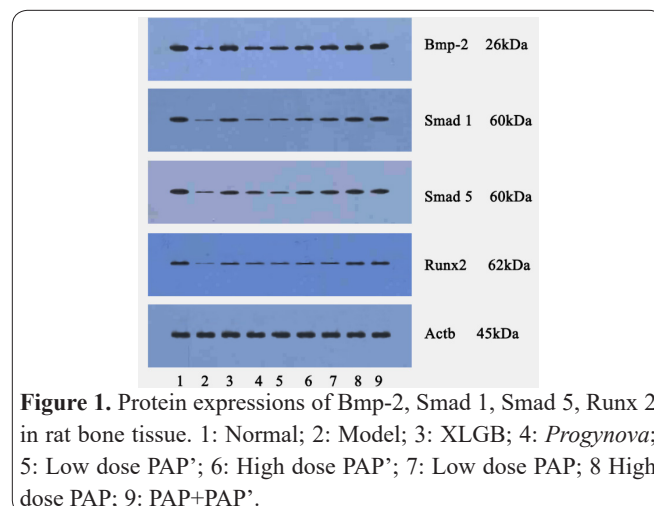


Figure 1. Protein expressions of Bmp-2, Smad 1, Smad 5, Runx 2 in rat bone tissue. 1: Normal; 2: Model; 3: XLGB; 4: *Prodynova*; 5: Low dose PAP; 6: High dose PAP; 7: Low dose PAP; 8 High dose PAP; 9: PAP+PAP'.

Table 3. Effect of treatments on ALP, BGP, BMP-2, E2, TRAP, PPAR γ -2 proteins in rat serum (n=10, $\bar{x}\pm s$).

Group	ALP (U/L)	BGP (ug/L)	BMP-2 (ug/L)	E2 (ng/L)	TRACP (pg/L)	PPAR γ -2 (ng/L)
Normal	101.918 \pm 0.646	231.489 \pm 3.344	220.734 \pm 4.882	97.171 \pm 0.979	84.919 \pm 1.016	85.929 \pm 1.394
Model	62.651 \pm 2.07 ^Δ	122.846 \pm 1.33 ^Δ	120.763 \pm 2.578 ^Δ	57.899 \pm 2.021 ^Δ	130.189 \pm 2.185 ^Δ	133.334 \pm 2.87 ^Δ
Prodynova	79.591 \pm 0.904 [#]	170.801 \pm 2.723 [#]	179.546 \pm 3.35 [#]	73.212 \pm 1.15 [#]	104.979 \pm 2.523 [#]	105.858 \pm 1.819 [#]
XLGB	114.525 \pm 1.984 [#]	165.002 \pm 3.833 [#]	166.106 \pm 3.09 [#]	110.799 \pm 2.796 [#]	99.405 \pm 2.671 [#]	101.420 \pm 2.704 [#]
PAP+PAP'	94.91 \pm 1.752 ^{*#}	226.731 \pm 4.202 ^{*#}	217.929 \pm 3.137 ^{*#}	89.467 \pm 1.341 ^{*#}	94.978 \pm 2.039 ^{*#}	97.862 \pm 6.412 ^{*#}
Low dose PAP	82.512 \pm 1.511 ^{*#}	159.230 \pm 3.344 ^{*#}	153.457 \pm 3.369 ^{*#}	77.310 \pm 1.257 ^{*#}	106.450 \pm 4.733 ^{*#}	105.748 \pm 3.136 ^{*#}
High dose PAP	85.254 \pm 1.245 ^{*#}	167.645 \pm 3.696 ^{*#}	165.829 \pm 3.408 ^{*#}	85.458 \pm 10.278 ^{*#}	100.316 \pm 4.27 ^{*#}	103.833 \pm 8.267 ^{*#}
Low dose PAP'	69.391 \pm 1.196 ^{*#}	138.343 \pm 1.788 ^{*#}	131.68 \pm 2.649 ^{*#}	65.43 \pm 1.317 ^{*#}	122.025 \pm 1.527 ^{*#}	125.782 \pm 3.564 ^{*#}
High dose PAP'	74.824 \pm 1.78 ^{*#}	150.019 \pm 2.149 ^{*#}	142.592 \pm 2.763 ^{*#}	71.464 \pm 1.475 ^{*#}	115.085 \pm 1.761 ^{*#}	116.336 \pm 2.623 ^{*#}

* $p < 0.05$, compared with the positive group, # $p < 0.05$, compared with the model group; ^Δ $p < 0.05$, compared with the normal group.

Table 4. Effect of various treatments on BALP, BMP-2, Smad 1, Smad 5, Runx 2, TGF- β 1 proteins in bone tissue (n=10, $\bar{x}\pm s$).

Group	BALP (ug/L)	BMP-2 (ug/L)	Smad 1 (ng/L)	Smad 5 (ng/L)	Runx 2 (ng/L)	TGF- β 1 (ng/L)
Normal	144.14 \pm 4.448	132.314 \pm 4.662	128.446 \pm 35.623	175.590 \pm 2.086	159.245 \pm 2.188	133.428 \pm 2.616
Model	93.261 \pm 5.122 ^Δ	73.309 \pm 4.415 ^Δ	69.789 \pm 20.343 ^Δ	94.873 \pm 1.588 ^Δ	83.072 \pm 1.877 ^Δ	63.389 \pm 1.304 ^Δ
Prodynova	101.462 \pm 2.952 [#]	91.419 \pm 2.183 [#]	97.260 \pm 20.607 [#]	111.537 \pm 3.991 [#]	102.933 \pm 1.978 [#]	82.015 \pm 0.992 [#]
XLGB	125.913 \pm 3.025 [#]	132.486 \pm 2.774 [#]	106.115 \pm 10.42 [#]	126.405 \pm 3.685 [#]	110.029 \pm 2.500 [#]	96.239 \pm 1.366 [#]
PAP+PAP'	123.16 \pm 2.436 ^{*#}	115.378 \pm 3.088 ^{*#}	142.42 \pm 15.482 ^{*#}	165.583 \pm 4.279 ^{*#}	151.071 \pm 3.224 ^{*#}	109.883 \pm 1.955 ^{*#}
Low dose PAP	104.299 \pm 3.764 ^{*#}	93.785 \pm 2.163 ^{*#}	99.782 \pm 9.934 ^{*#}	115.478 \pm 4.336 ^{*#}	87.285 \pm 2.511 ^{*#}	80.272 \pm 2.988 ^{*#}
High dose PAP	92.256 \pm 3.514 ^{*#}	104.032 \pm 3.303 ^{*#}	116.378 \pm 13.339 ^{*#}	128.038 \pm 3.803 ^{*#}	129.969 \pm 3.550 ^{*#}	96.543 \pm 2.564 ^{*#}
Low dose PAP'	93.068 \pm 2.549 ^{*#}	84.846 \pm 1.493 ^{*#}	88.808 \pm 9.94 ^{*#}	103.367 \pm 3.716 ^{*#}	91.749 \pm 4.712 ^{*#}	72.579 \pm 1.644 ^{*#}
High dose PAP'	100.73 \pm 2.49 ^{*#}	94.559 \pm 1.243 ^{*#}	94.093 \pm 8.359 ^{*#}	107.109 \pm 1.718 ^{*#}	98.186 \pm 1.902 ^{*#}	76.163 \pm 1.393 ^{*#}

* $p < 0.05$, compared with the positive group, # $p < 0.05$, compared with the model group; ^Δ $p < 0.05$, compared with the normal group.

Table 5. Effect of various treatments on the mRNA expressions of Bmp-2, Smad 1, Smad 5 and Runx 2 in bone tissue (n=10, $\bar{x}\pm s$).

Group	Bmp-2	Smad 1	Smad 5	Runx 2
Normal	1.00 \pm 0.03	1.00 \pm 0.10	1.00 \pm 0.02	1.00 \pm 0.03
Model	0.51 \pm 0.05 ^Δ	0.55 \pm 0.07 ^Δ	0.40 \pm 0.03 ^Δ	0.44 \pm 0.05 ^Δ
Prodynova	0.63 \pm 0.05 [#]	0.56 \pm 0.09 [#]	0.54 \pm 0.04 [#]	0.50 \pm 0.02 [#]
XLGB	0.90 \pm 0.05 [#]	0.72 \pm 0.08 [#]	0.66 \pm 0.04 [#]	0.64 \pm 0.04 [#]
PAP+PAP'	0.93 \pm 0.03 ^{*#}	0.97 \pm 0.11 ^{*#}	0.89 \pm 0.04 ^{*#}	0.91 \pm 0.03 ^{*#}
Low dose PAP	0.73 \pm 0.04 ^{*#}	0.74 \pm 0.06 ^{*#}	0.65 \pm 0.03 ^{*#}	0.57 \pm 0.04 ^{*#}
High dose PAP	0.82 \pm 0.03 ^{*#}	0.82 \pm 0.05 ^{*#}	0.76 \pm 0.04 ^{*#}	0.80 \pm 0.04 ^{*#}
Low dose PAP'	0.62 \pm 0.04 ^{*#}	0.59 \pm 0.07 ^{*#}	0.50 \pm 0.03 ^{*#}	0.53 \pm 0.03 ^{*#}
High dose PAP'	0.76 \pm 0.03 ^{*#}	0.65 \pm 0.08 ^{*#}	0.55 \pm 0.04 ^{*#}	0.61 \pm 0.03 ^{*#}

* $p < 0.05$, compared with the positive group, # $p < 0.05$, compared with the model group; ^Δ $p < 0.05$, compared with the normal group.

Table 6. Effect of various treatments on the protein expressions of Bmp-2, Smad 1, Smad 5 and Runx 2 in bone tissue (n=10, $\bar{x}\pm s$).

Group	BMP-2	Smad 1	Smad 5	Runx 2
Normal	1.058±0.059	0.876±0.079	0.844±0.085	0.658±0.055
Model	0.404±0.021 ^Δ	0.212±0.036 ^Δ	0.256±0.023 ^Δ	0.21±0.034 ^Δ
Progynova	0.626±0.039 [#]	0.288±0.022 [#]	0.468±0.046 [#]	0.332±0.050 [#]
XLGB	0.972±0.104 [#]	0.574±0.054 [#]	0.610±0.067 [#]	0.38±0.061 [#]
PAP+PAP'	1.040±0.053 ^{*#}	0.790±0.092 ^{*#}	0.768±0.139 ^{*#}	0.3969±0.153 ^{*#}
Low dose PAP	0.830±0.048 ^{*#}	0.540±0.040 ^{*#}	0.604±0.065 ^{*#}	0.328±0.045 ^{*#}
High dose PAP	0.980±0.057 ^{*#}	0.720±0.055 ^{*#}	0.744±0.077 ^{*#}	0.544±0.062 ^{*#}
Low dose PAP'	0.616±0.040 ^{*#}	0.3385±0.016 ^{*#}	0.342±0.052 ^{*#}	0.3360±0.044 ^{*#}
High dose PAP'	0.810±0.054 ^{*#}	0.462±0.0303 ^{*#}	0.516±0.058 ^{*#}	0.3060±0.052 ^{*#}

**p* < 0.05, compared with the positive group, #*p* < 0.05, compared with the model group; ^Δ*p* < 0.05, compared with the normal group.

Table 7. Mean optical density of proteins in bone tissue (n=10, $\bar{x}\pm s$).

Group	Bmp-2	Smad1	Smad5	Runx2
Normal	0.164±0.035	0.1675± 0.057	0.130±0.028	0.207±0.071
Model	0.15±0.035 ^Δ	0.119±0.033 ^Δ	0.109±0.024 ^Δ	0.175±0.044 ^Δ
XLGB	0.188±0.059 [#]	0.153± 0.067 [#]	0.169±0.124 [#]	0.235±0.038 [#]
Progynova	0.165±0.057 [#]	0.124±0.031 [#]	0.22±0.098 [#]	0.188±0.021 [#]
PAP+PAP'	0.188±0.059 ^{*#}	0.281±0.079 ^{*#}	0.161±0.028 ^{*#}	0.226±0.018 ^{*#}
Low dose PAP	0.160±0.039 ^{*#}	0.141 ± 0.071 ^{*#}	0.106±0.016 ^{*#}	0.223±0.033 ^{*#}
High dose PAP	0.167 ± 0.038 ^{*#}	0.147 ± 0.074 ^{*#}	0.133± 0.050 ^{*#}	0.214±0.049 ^{*#}
Low dose PAP'	0.151±0.023 ^{*#}	0.155±0.046 ^{*#}	0.134±0.023 ^{*#}	0.246±0.054 ^{*#}
High dose PAP'	0.161± 0.028 ^{*#}	0.161±0.067 ^{*#}	0.081± 0.018 ^{*#}	0.241±0.035 ^{*#}

**p* < 0.05, compared with the positive group, #*p* < 0.05, compared with the model group; ^Δ*p* < 0.05, compared with the normal group.

Effect of various treatments on bone metabolism-related genes and proteins

As shown in Tables 5 & 6 and Figure 1, the mRNA and protein expression levels of Bmp-2, Smad 1, Smad 5 and Runx 2 were significantly decreased (*p* < 0.05). However, treatment with *Pilose antler* increased the mRNA and protein expression levels of these genes.

Immunohistochemistry

The results of immunohistochemistry are shown in Table 7 and in Figures 2, 3, 4 and 5 (immunohistochemistry staining results of Bmp-2, Smad 1, Smad 5 and

Runx 2, respectively).

Discussion

Selection of animal models for osteoporosis

It has been repeatedly demonstrated that osteoporotic models in ovariectomized female rats have become well-accepted standard pathological models of post-menopausal osteoporosis. Menopausal osteoporosis in terms of its clinical performance, and Traditional Chinese Medicine (TCM) concepts of "bone sputum", "kidney low back pain" and "bone withered" mainly in-

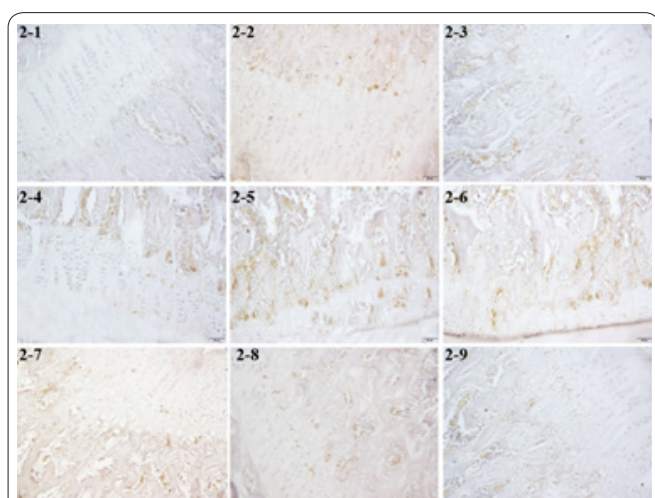


Figure 2. Immunohistochemistry staining results for Bmp-2. 1: normal group; 2: model group; 3: XLGB group; 4: *Progynova* group; 5: Low dose polypeptide group; 6: High dose polypeptide group; 7: Low dose polysaccharide group; 8: High dose polysaccharide group; 9: polypeptide + polysaccharide group.

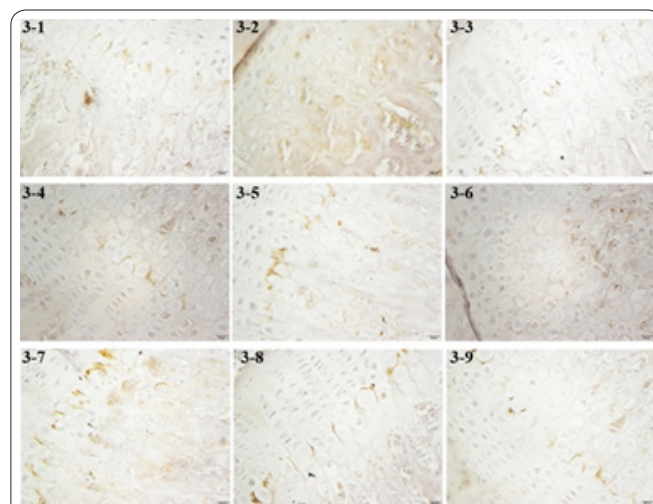


Figure 3. Immunohistochemistry staining results for Smad 1. 1: normal group; 2: model group; 3: XLGB group; 4: *Progynova* group; 5: Low dose polypeptide group; 6: High dose polypeptide group; 7: Low dose polysaccharide group; 8: High dose polysaccharide group; 9: polypeptide + polysaccharide group.

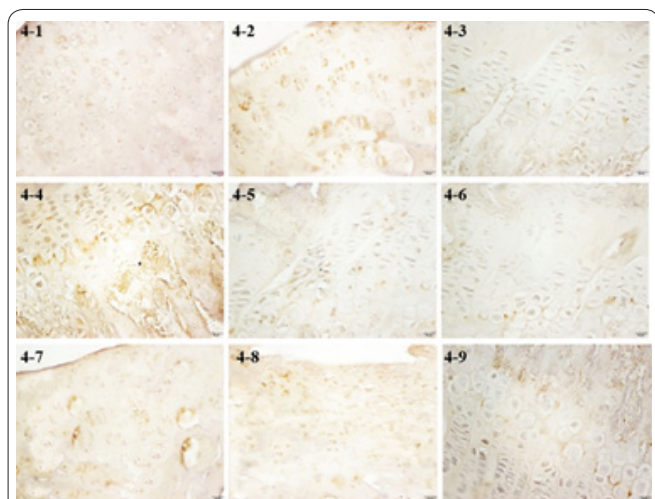


Figure 4. Immunohistochemistry staining results for Smad 5. 1: normal group; 2: model group; 3: XLGB group; 4: *Progynova* group; 5: Low dose polypeptide group; 6: High dose polypeptide group; 7: Low dose polysaccharide group; 8: High dose polysaccharide group; 9: polypeptide + polysaccharide group.

involve kidney deficiency. In this study, the postmenopausal osteoporosis model was replicated by removing the bilateral ovaries of female rats, i.e. the *kidney deficiency* osteoporosis model in TCM theory. After the removal of bilateral ovaries, rats in the model group developed paralysis of the back of the bow, which is in line with one of the main symptoms of the TCM kidney deficiency in experimental animal models. The rat femur BMD was significantly lower than that of the normal group. The uterine index was also significantly lower, when compared with the normal group. The experimental results showed that the rats in the model group had pathological features of *kidney deficiency* osteoporosis, which proved that the rat model of kidney deficiency osteoporosis caused by removal of the ovary was successfully established/replicated.

To discuss the substance basis of pilose antler for osteoporosis

From the results of this study, it can be seen that compared with the model group, treatment in each group significantly increased serum estradiol (E2), alkaline phosphatase (ALP), osteocalcin (BGP), bone morphogenetic protein-2 (BMP-2), tartrate-resistant acid phosphatase (TRAP) receptor γ -2 (PPAR γ -2), bone-derived alkaline phosphatase (BALP), and BMP in bone tissue. Moreover, the mRNA and protein expression levels of BMP-2, Smad 1, Smad 5, and Runx 2 in bone tissue were increased. Although *Pilose antler* polypeptides and polysaccharides increased the levels of serum test markers in rats and increased the expressions of related proteins, the effect of combination of the polypeptides and polysaccharides was even more significant in some measurement indicators which were significantly higher than those in the positive control group. The polypeptides and polysaccharides in *Pilose antler* are the material bases for the *kidney tonifying* and bone strengthening effects of *Pilose antler*. The polypeptide group was more effective than the polysaccharide group, but the combination treatment was more effective than when either of them was used alone. The active principle comprised the organic integration of the

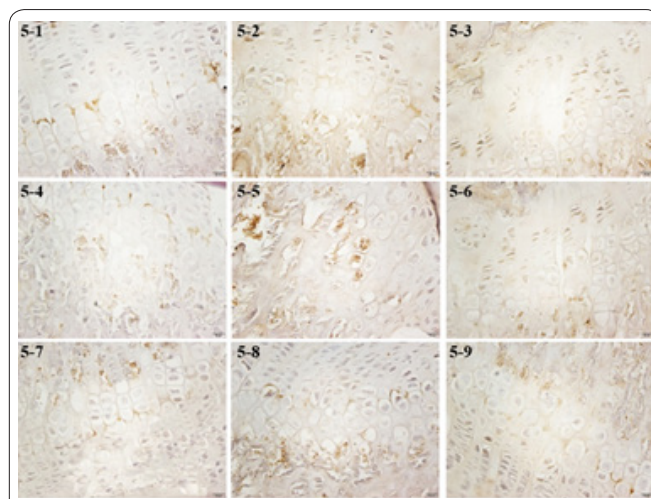


Figure 5. Immunohistochemistry staining results for Runx 2. 1: normal group; 2: model group; 3: XLGB group; 4: *Progynova* group; 5: Low dose polypeptide group; 6: High dose polypeptide group; 7: Low dose polysaccharide group; 8: High dose polysaccharide group; 9: polypeptide + polysaccharide group.

effects of various components. The proportions of polypeptide and polysaccharide in *Pilose antler* will be the subject of further studies.

Studies on the mechanism underlying the treatment of osteoporosis with Pilose antler

Stromal cells isolated from bone marrow can be induced to differentiate into cells possessing the characteristics of mature osteoblast (14). Bone formation requires three essential steps viz: osteoblast differentiation, matrix maturation and matrix mineralization (15). The process is characterized by cellular expression and synthesis of bone marker proteins for matrix maturation, and by extracellular matrix mineralization triggered by calcium deposition (16). Alkaline phosphatase (ALP) is the transporter protein that binds with calcium, and it promotes cell maturation and calcification, while BGP is a necessary factor for bone calcification. These two factors are markers of differentiation in the early and middle stages (17). One of the most powerful osteogenesis-promoting proteins is BMP-2 (18-21). During osteoblast differentiation, BMP-2 is bound to 2 types of serine/threonine kinase receptors-bmpr i.e. type I and type II to initiate the BMP signaling pathway (22-25). Firstly, BMP induces the activation of receptor-regulated Smads (R-Smad; Smad1, Smad 5, and Smad 8), and regulation of target genes such as OPN, BGP, ALP, and Runx 2 (26, 27). The present study found that the levels of ALP, BGP, BMP-2 in both PAP group and the inducing medium group were significantly higher than those in the control group. This demonstrates that PAP not only enhanced proliferation of BMSCs but also promoted BMSCs to differentiate into osteoblasts. Further research will be necessary to assess the effect of PAP on bone regeneration and its therapeutic potential in bone formation *in vivo*.

The BMP-2 and ALP are specific indicators of osteoblasts. Studies have shown that BGP is an important component of non-collagenous bone matrix involved maintenance of normal bone mineralization rate and promotion of normal calcification of bone tissue (11). The enzyme TRAP is closely related to the degrada-

tion of bone matrix secreted by osteoclasts. The level of TRAP in serum indicates the degree of bone resorption (11). Research has shown that PPAR γ -2 plays an important role in the regulation process of conversion between osteoblasts and osteoclasts and bone mass, and is closely related to osteoporosis. The BMSCs were affected by PPAR γ -2 factor in the process of differentiation into adipocytes (28, 29). When the number of adipocytes in the marrow cavity increases and the number of osteoblasts in the marrow cavity decreases, resulting in imbalance in the proportion of these two cells, the bone morphological structure changes, leading to osteoporosis (30, 31).

The most abundant growth factor in bone is TGF- β . It regulates the proliferation and differentiation of osteoblasts, stimulation of collagen and bone matrix protein synthesis. A member of the TGF- β superfamily, TGF- β 1 has the most intimate relationship with bone formation. It is a potential factor for bone induction process, and one of the preferred growth factors regulating osteogenic differentiation (32-34).

It is known that BMP-2 is one of the most important extracellular signaling molecules that promote bone formation and osteoblast differentiation. It plays a role in osteogenesis by activating Smads signaling and regulating the transcription of osteogenic genes. The Smad family comprises about 9 BMP signaling proteins, of which Smad 2 and Smad 3 can transfer TGF- β activin signal, while Smad 1, Smad 5, Smad 8 and Smad 9 regulate BMP signal transduction. The Smads are activated by BMP which induces their expressions in the nucleus (11). The Runxs are specific transcription factors that regulate the differentiation of mesenchymal stem cells into osteoblasts. They comprise Runx 1, Runx 2 and Runx 3. In particular, Runx 2 is the target gene of BMP-2. It is an important regulator of BMSC and osteoblasts (OB) differentiation and bone development, and plays an important role in osteoblast differentiation. When BMP-2 activates Smad 1, Smad 5, and Smad 8, the expression of Runx 2 gene is activated by its distal P1 promoter and the proximal P2 promoter. The level of functional Runx 2 determines the degree of bone maturation and conversion.

Therefore, Pilose antler had some preventive effects on osteoporosis, probably via the activation of the Bmp-2/Smad1 and Smad5/Runx2 signaling pathways through induction of high expressions of their mRNAs and proteins.

Acknowledgments

This study was supported by the National Natural Science Foundation of China (grant No.81473314).

Conflict of Interest

There are no conflict of interest in this study.

Author's contribution

All work was done by the authors named in this article and the authors accept all liability resulting from claims which relate to this article and its content. The study was conceived and designed by Feng Li; Cong Ren, Wei Gong, Feng Li and Ming Xie collected and analysed the data; Cong Ren wrote the text and all authors have read and approved the text prior to publication.

References

1. Wang BM, Zhao N, Yu HY, Xu HT. Research progress of Chinese and western medicine in osteoporosis. *Chin Med Inf* 2016; 33: 128-131.
2. Liu ZH. Osteoporosis (first edition). Science Press, Beijing, 1998, pp. 142.
3. Feng LK, Zhu JY, Yao HM. Progress of traditional Chinese medicine therapy for osteoporosis. *J Tonghua Normal Univ* 2019; 40: 51-55.
4. Deng C, Zhou MW, Fu ZB, Li SH. TCM etiology, pathogenesis and treatment progress of osteoporosis. *Chin J Osteoporos* 2017; 23: 1105-1111.
5. Li HF, Zhou WS. Progress in the pathogenesis of osteoporosis in Chinese and Western medicine. *Mod Clin Med Bioeng Mag* 2003; 9: 450-455.
6. Wang HF, Weng SF. Bone mineral density measurement in rats and its application in the establishment of osteoporosis model. *Chin J Osteoporos* 1995; 2: 8-9.
7. Li YH, Dang XQ, Gong FT, Ban WR, Ma J, Shi YW, et al. Research progress and literature review of animal models of osteoporosis. *Tissue Eng Res China* 2008; 22: 1956-1961.
8. Lindsay R, Tohme JF. Estrogen treatment of patients with established postmenopausal osteoporosis. *Obstet Gynecol* 1990; 76: 290-295.
9. Luo T, Gao Y, Yin YH, Xu L. Research status of traditional Chinese medicine on osteoporosis. *Hunan J Tradit Chin Med* 2014; 30: 148-149.
10. National Pharmacopoeia Committee, Volume One, Chinese Pharmacopoeia, 2015 Edition, Beijing, The Medicine Science and Technology Press of China, 2015, pp. 323-324.
11. Gong W. Study on the relationship between the role of "tonifying the kidney and strengthening bone" and the quality of the Pilose Antler. *Liaoning Univ Tradit Chin Med* 2011.
12. Ye J, Coulouris G, Zaretskaya I, Cutcutache I, Rozen S, Madden TL. Primer-BLAST: A tool to design target-specific primers for polymerase chain reaction. *BMC Bioinform* 2012; 13: 134.
13. Pfaffl MW. A new mathematical model for relative quantification in real-time RT-PCR. *Nucleic Acids Res* 2001; 29: 2002-2007.
14. Kobune M, Kato J, Chiba H, Kawano Y, Tanaka M, Takimoto R, et al. Telomerized human bone marrow-derived cell clones maintain the phenotype of hematopoietic-supporting osteoblastic and myofibroblastic stromal cells after long-term culture. *Exp Hematol* 2005; 33: 1544-1553.
15. Komori T. Regulation of bone development and maintenance by Runx2. *Front Biosci* 2008; 13: 898-903.
16. Gaur T, Hussain S, Mudhasani R, Parulkar I, Colby JL, Frederick D, et al. Dicer inactivation in osteoprogenitor cells compromises fetal survival and bone formation, while excision in differentiated osteoblasts increases bone mass in the adult mouse. *Dev Biol* 2010; 340: 10-21.
17. Hu ZM, Peel SA, SK HO, Sandor GK, Clokie CM. Induction of bone matrix protein expression by native bone matrix proteins in C2C12 culture. *Biomed Environ Sci* 2009; 22: 164-169.
18. Smoljanovic T, Bojanic I, Bogovic M. Bone morpho-genetic protein. *J Neurosurg Spine* 2012; 11: 92-93.
19. Lo KW, Ulery BD, Ashe KM, Laurencin CT. Studies of bone morphogenetic protein-based surgical repair. *Adv Drug Deliv Rev* 2012; 64: 1277-1291.
20. Kato S, Kawabata N, Suzuki N, Ohmura M, Takagi M. Bone morphogenetic protein-2 induces the differentiation of a mesenchymal progenitor cell line, ROB-C26, into mature osteoblasts and adipocytes. *Life Sci* 2009; 84: 302-310.
21. Karageorgiou V, Meinel L, Hofmann S, Malhotra A, Volloch

V, Kaplan D. Bone morpho-genetic protein-2 decorated silk fibroin films induce osteogenic differentiation of human bone marrow stromal cells. *J Biomed Mater Res A* 2004; 71: 528-537.

22. Tachi K, Takami M, Zhao B, Mochizuki A, Yamada A, Miyamoto Y, et al. Bone morphogenetic protein 2 enhances mouse osteoclast differentiation via increased levels of receptor activator of NF- κ B ligand expression in osteoblasts. *Cell Tissue Res* 2010; 342: 213-220.

23. Cao X, Chen D. The BMP signaling and in vivo bone formation. *Gene* 2005; 357: 1-8.

24. ten Dijke P. Bone morphogenetic protein signal transduction in bone. *Curr Med Res Opin* 2006; 22: 7-11.

25. Franceschi RT, Ge C, Xiao G, Roca H, Jiang D. Transcriptional Regulation of Osteoblasts. *Cells Tissues Organs* 2009; 189: 144-152.

26. Gong W, Li F. Cervi cornu pantotrichum aqueous extract promote osteoblasts differentiation and bone formation. *Biomed Res* 2014; 25: 249-252.

27. Yeung DKW, Griffith JF, Antonio GE, Lee FKH, Woo J, Leung PC. Osteoporosis is associated with increased marrow fat content and decreased marrow fat unsaturation: a proton 27.MR spectroscopy study. *J Magn Reson Imaging* 2010; 2: 279-285.

28. Li CQ. Screening for the anti-inflammatory activity of fractions and compounds from *Atractylodesmacrocephala koidz.* *J Ethnopharmacol* 2007; 114: 212-217.

29. JC Lee, KY Lee, YO Son, KC Choi, J Kim, SH Kim, et al. Stimulating effects on mouse Spleucocytes of glyco-proteins from the herbal medicine *Atractylodes macrocephala* Koidz. *Phytomed* 2007; 14: 390-395.

30. Shi CD, Yang YH, Yu X, Zhang RQ, Wang XL, Nie AD. Effect of Kangshu Jiangu Granules on the Expression of PPAR γ -2 of Bone Tissue from Ovariectomized Osteoporosis Model Rats. *J Sichuan Tradit Chin Med* 2015; 33: 61-64.

31. Hu J, Zhang AB, Liu XL, Zhou JN. Extracorporeal shock wave promotes differentiation of human bone marrow stromal cells into osteoprogenitors. *Chin J Exp Surg* 2005; 22: 147-150.

32. Sun WP, Li FS, Chen C, Luo H, Yang G, Liu H. Immunomodulation of *Atractylodes* polysaccharides in mice. *Chin J Microecol* 2011; 23: 881-882, 886.

33. Kim K, Dean D, Wallace J, Breithaupt R, Mikos AG, Fisher JP. The influence of stereolithographic scaffold architecture and composition on osteogenic signal expression with rat bone marrow stromal cells. *Biomater* 2001; 32: 3750.

34. Ren YL, Li YL, Lv HB, Liu LP, Zhao JR, Wang LC. Expressions of TGF- β 1/Smad4 mRNA of Kidney by Zuogui Pill in Ovariectomy-induced Osteoporosis Rats. *Chin J Exp Tradit Med Form* 2012; 10: 190-194.